FEBS Letters 579 (2005) 1376–1382 FEBS 29291

Structure of a type II thymidine kinase with bound dTTP

Markus S. Birringer[a], Michael T. Claus[b], Gerd Folkers[a], Daniel P. Kloer[b], Georg E. Schulz[b], Leonardo Scapozza[a,*]

[a] *Institute of Pharmaceutical Sciences, Department of Chemistry and Applied Biosciences, Swiss Federal Institute of Technology (ETH), Wolfgang-Pauli Strasse 10, 8093 Zurich, Switzerland*

[b] *Institut für Organische Chemie und Biochemie, Albert–Ludwigs–Universität, Albertstrasse 21, 79104 Freiburg im Breisgau, Germany*

Received 30 September 2004; revised 6 December 2004; accepted 9 January 2005

Available online 30 January 2005

Edited by Christian Griesinger

Abstract The structure of human cytosolic thymidine kinase in complex with its feedback inhibitor 2′-deoxythymidine-5′-triphosphate was determined. This structure is the first representative of the type II thymidine kinases found in several pathogens. The structure deviates strongly from the known structures of type I thymidine kinases such as the Herpes simplex enzyme. It contains a zinc-binding domain with four cysteines complexing a structural zinc ion. Interestingly, the backbone atoms of the type II enzyme bind thymine via hydrogen-bonds, in contrast to type I, where side chains are involved. This results in a specificity difference exploited for antiviral therapy. The presented structure will foster the development of new drugs and prodrugs for numerous therapeutic applications.

Keywords: Human thymidine kinase; Antiviral drugs; dTTP; Cancer; Suicide gene; Zinc finger

1. Introduction

Using ATP, thymidine kinases catalyze the phosphorylation of 2′-deoxythymidine (dT) within the so-called pyrimidine salvage-pathway. These kinases have been classified into type I (long) and type II (short) subfamilies. The human cytosolic enzyme (hTK1) belongs to the type II while the Herpes simplex virus 1 enzyme, whose structure is known, represents type I. hTK1 is highly specific accepting only dT-analogs with restricted changes in the sugar moiety [1]. In contrast, the substrate specificity of type I subfamily is rather broad [2]. This difference in specificity is the basic principle for the selectivity of the established antiviral therapy using aciclovir and its derivatives [3].

The type II thymidine kinases (TK) show very low sequence similarity with the type I enzymes and other established nucleoside kinases rendering model building virtually impossible. They occur in many different organisms like bacteria (*Staphylococcus aureus*, *Bacillus anthracis*, *Mycoplasma pneumoniae*), eukaryotes (*Leishmania major*, *Trypanosoma brucei*) and viruses (*Cowpox*, *Vaccinia*, *Variola*, *Swinepox*) that are likely targets for therapeutic intervention. We suggest that the structure of hTK1 allows to produce reasonably accurate models of the thymidine kinases of these organisms such that drugs and prodrugs can be developed. The ability of type II TK of activating prodrugs is already documented for HIV therapy. Here, hTK1 activates the prodrug 3′-azido-2′,3′-dideoxy-thymidine (AZT) that, in its triphosphorylated form, becomes an inhibitor of the HIV reverse transcriptase.

Circumventing the cell growth inhibitory effect of chemotherapeutics like methotrexate that interfere with the pyrimidine biosynthesis pathway, tumor cells use the pyrimidine salvage pathway to continue proliferation [4]. This may be prevented by adding hTK1 inhibitors as adjuvant for chemotherapeutics. Such inhibitors can now be designed in the light of the known structure since the missing structural information on type II enzymes prevented their development so far. Moreover, hTK1 has been used for the localization of tumors and metastasis with positron emission tomography (PET) in combination with ^{18}F-labeled dT [5–7]. This PET tracer is taken up by highly proliferating cells that show an increased hTK1 activity. It is then phosphorylated accumulating a PET signal to be used for tumor localization. Although, ^{18}F-labeled dT has been used in patients some problems related to liver accumulation and low blood-brain barrier passage have been observed [7]. Thus, there is a need for improved PET tracers for hTK1 and these can now be ameliorated in a directed manner.

Herpes viral thymidine kinase is presently used as suicide gene in therapies based on stem cell transplantation to control them in case of adverse effects such as graft versus host disease [8,9]. Unfortunately, immunogenic epitopes of the Herpes enzyme are presented at the cell surface causing elimination by T-cells and thus loss of the transplanted stem cells resulting in treatment failure. Now the structure of hTK1 allows engineering toward a non-immunogenic human suicide gene to replace the Herpes enzyme overcoming the encountered problems [10]. Taken together the presented structure concerns an enzyme that is deeply involved in various modern therapeutic approaches.

2. Materials and methods

2.1. Crystallization

The hTK1 was cloned as N-terminal thrombin-cleavable His_6-tagged fusion protein missing 14 amino acids of the N-terminus and 40 amino acids of the C-terminus of the wild type hTK1 sequence of 234 amino acids (this construct is further on called

*Corresponding author. Present address: Laboratoire de Chimie Thérapeutique, Section des Sciences Pharmaceutiques, Université de Genève, Quai Ernest-Ansermet 30, 1211 Genève 4, Switzerland.
E-mail address: leonardo.scapozza@pharm.unige.ch (L. Scapozza).

Abbreviations: hTK1, human cytosolic thymidine kinase; dT, 2′-deoxythymidine; dTTP, 2′-deoxythymidine-5′-triphosphate; MAD, multi-wavelength anomalous diffraction

0014-5793/$30.00
doi:10.1016/j.febslet.2005.01.034

hTK1). The purified hTK1, consisting of residues 15–194 of the wild type sequence plus an N-terminal extension of 15 residues containing a His_6-tag, was eluted from gel filtration column at a concentration of approximate 7 mg/ml with a buffer containing 5 mM Tris at pH 7.2, 10 mM NaCl and 10 mM DTT. For protein crystallization we used the hanging drop method at 23 °C. Initial conditions for crystallization were found using Crystal screen Cryo no. 40 (Hampton Research). The protein solution was mixed in a 1:1 ratio with crystallization buffer (0.095 mM tri-sodium citrate, pH 5.5, 12% PEG 4000, 10% isopropanol) to set up drops of 6 μl. The reservoir contained 500 μl of crystallization buffer.

Crystals appeared after 3 days and grew within 3 days to sizes of about $300 \times 150 \times 70\ \mu m^3$ and diffracted to 1.7 Å resolution. They belong to space group C2 with $a = 157.5$ Å, $b = 122.9$ Å, $c = 115.3$ Å, $\alpha = \gamma = 90°$ and $\beta = 130°$. The asymmetric unit contains 8 monomers forming two tetramers. The solvent content is 48%. For X-ray data collection the crystals were cryo-protected using crystallization buffer with additional 30% glycerol soaking for one minute. The crystals diffract up to 1.7 Å resolution and are stable under X-radiation from beamline X06SA at Swiss Light Source (Villigen/CH).

2.2. Data collection, phase determination and refinement

Three datasets were collected from two crystals. A fluorescence scan from one crystal was performed and data were collected at two wavelengths ($\lambda = 1.2776$ Å (zinc edge) and 0.9196 Å). The data processing was performed with the program XDS [11]. These data sets were used for multi-wavelength anomalous diffraction (MAD) phasing. The zinc coordinates were determined with program CNS [12]. Initial two wavelength MAD phases to 4 Å were obtained with SHARP [13] and extended to 1.83 Å by 8-fold NCS averaging, solvent flattening and histogram matching implemented in RESOLVE [14] using the third data set ($\lambda = 0.9793$ Å) collected from the second crystal. An initial model was obtained with RESOLVE, which was subsequently rebuilt and refined with XFIT [15] and REFMAC [16], respectively. Model refinement was started using NCS restraints, which were stepwise released and finally omitted. Water molecules were introduced using ARP_WATERS [16] when the *R*-factor reached 20%. Refinement results were checked with PROCHECK [17] and WHATCHECK [18]. Coordinates and structure factors have been deposited in the Brookhaven Protein Data Bank (Accession code 1w4r). The figures were produced with POVScript+ [19]. For secondary structure assignment DSSP [20] was used. The *B*-factor plot was calculated with BAVERAGE [16] and the density correlation was done with the program OVERLAPMAP [21]. The numbering of the hTK1 [EC 2.7.1.21] sequence corresponds to the hTK1 SwissProt entry P04183.

3. Results and discussion

Wild type hTK1 has 234 amino acids and forms a tetramer in solution [1]. The crystallized fragment consists of residues 15–194 plus an N-terminal extension of 15 residues containing a His_6-tag. This truncated form of hTK1 was designed to avoid protein precipitation during purification and corresponds in length to Vaccinia Virus TK (Fig. 1) that possess one of the shortest sequence among the type II TK. In contrast to the wild type hTK1, this truncated form is a dimer in solution (Supplementary material Fig. S6). Nevertheless, it conserved an intact thymidine kinase activity (Supplementary material Fig. S7) with a K_m value for dT of 0.8 ± 0.3 μM that is comparable to previously published K_m value of 0.5 μM for the wild type enzyme [22]. Similar to wild type enzyme, this truncated form of hTK1 is also inhibited by deoxythymidine-5′-triphosphate (dTTP) [23]. The enzyme (in complex with dTTP) crystallized in space group C2 with eight subunits per crystallographic asymmetric unit that form two D_2-symmetric tetramers (Fig. 2). Subunit A has the continuous chain from residues 18 to 191, whereas the other subunits have insufficient density for flexible residues 62–75. The structure was determined using zinc ion anomalous diffraction and refined to 1.83 Å resolution to good quality (Table 1). During the refinement a strong density appeared within a putative binding cavity in each subunit which was eventually identified as the feedback inhibitor dTTP (Fig. 3). Since dTTP was not present in the protein purification process or crystallization set up we assume that it originates from *E.coli* metabolism. The enzymatic activity of the expressed hTK1 in *E.coli* was most probably silenced by dTTP feedback inhibition preventing cell toxic effects and allowing a sustained expression of soluble protein.

The core of the protein contains a six stranded parallel β-sheet surrounded by five α- and four 3_{10}-helices (Figs. 2 and 4). In the chainfold of the enzyme four central β-strands with the P-loop and one connecting helix can be superimposed on other nucleoside and nucleotide kinases [24–26], while the rest of the main chain is substantially different.

```
HUMAN   15 ...sktRGQIQVILGPMFSGKSTELMRRVRRFQIAQYKCLVIKYAKDTRY-SSSFCTHDRNTME  74
VACCA    1     MNGGHIQLIIGPMFSGKSTELIRRVRRYQIAQYKCVTIKYSNDNRY-GTGLWTHDKNNFE  59
LEIMA    1     MFRGRIELIIGPMFAGKTTELMRRVKREIHARRSCFVIKYSKDTRYDEHNVASHDQLMLR  60
MYCPN    5 ...QSPRGWIEVICGPMFSGKTEELLRKIKRWKLAKIPVIIFKPKIDTRQQHLVKSRNGHSDEA  69
               ..:* *::* ****:**: **:*:::*   *:   . :*   *.*        :.:

HUMAN   75 ALPAC-LLRDVAQEALGVAVIGIDEGQFF-PDIVEFCEAMANAGKTVIVAALDGTFQRKPFGAI 135
VACCA   60 ALEAT-KLCDVLESITDFSVIGIDEGQFF-PDIVEFCERMANEGKIVIVAALDGTFQRKPFNNI 121
LEIMA   61 AQAAVSQLTEVRDTWKRFDVLAIDEGQFF-SDLVDFCNTAADAGKVVMVSALDGDYRRKPFGQI 123
MYCPN   70 IEINSPLEIYDYLTKDRFDVVAIDEAQFFSSEIVEVVKSLNDLGINVIVSGLDTDFRAEPFGSI 133
              .                . *:.***.*** .::*:. :   : *  *:*:.**  :: :**. *

HUMAN  136 LNLVPLAESVVKLTAVCMECFREAA-YTKRLGTEKEVEVIGGADKYHSVCRLCYFKkas...   194
VACCA  122 LNLIPLSEMVVKLTAVCMKCFKEAS-FSKRLGEETEIEIIGGNDMYQSVCRKCYVGS        177
LEIMA  124 CELVPYCEAVDKLTAVCMMCHEQPACFTRRTVNVEQQELIGGADMYIATCRECYSKQQL...   182
MYCPN  134 PQLLAIADKICKLDAVCNVCGQLAQRTQRIVSKSNETVLIGDIEAYEPRCKLHQPSAG       191
               :*:. .: : ** ***  * . :.   :       :  :**. : * . *: :
```

Fig. 1. Representative sequence alignment of hTK1 (SwissProt ID P04183) with other type II thymidine kinases from *Vaccinia virus* (O57203), *Leishmania major* (TrEMBL ID Q9N9I4) and *Mycoplasma pneumoniae* (P75070). Identical residues are highlighted by stars, conserved residues by dots. Residues which could be structurally aligned with Herpes viral thymidine kinase (PDB-code 1VTK) are underlined. They correspond to the yellow colored parts of Fig. 2B. Residues given in lower case were not modeled in hTK1 because of lacking density.

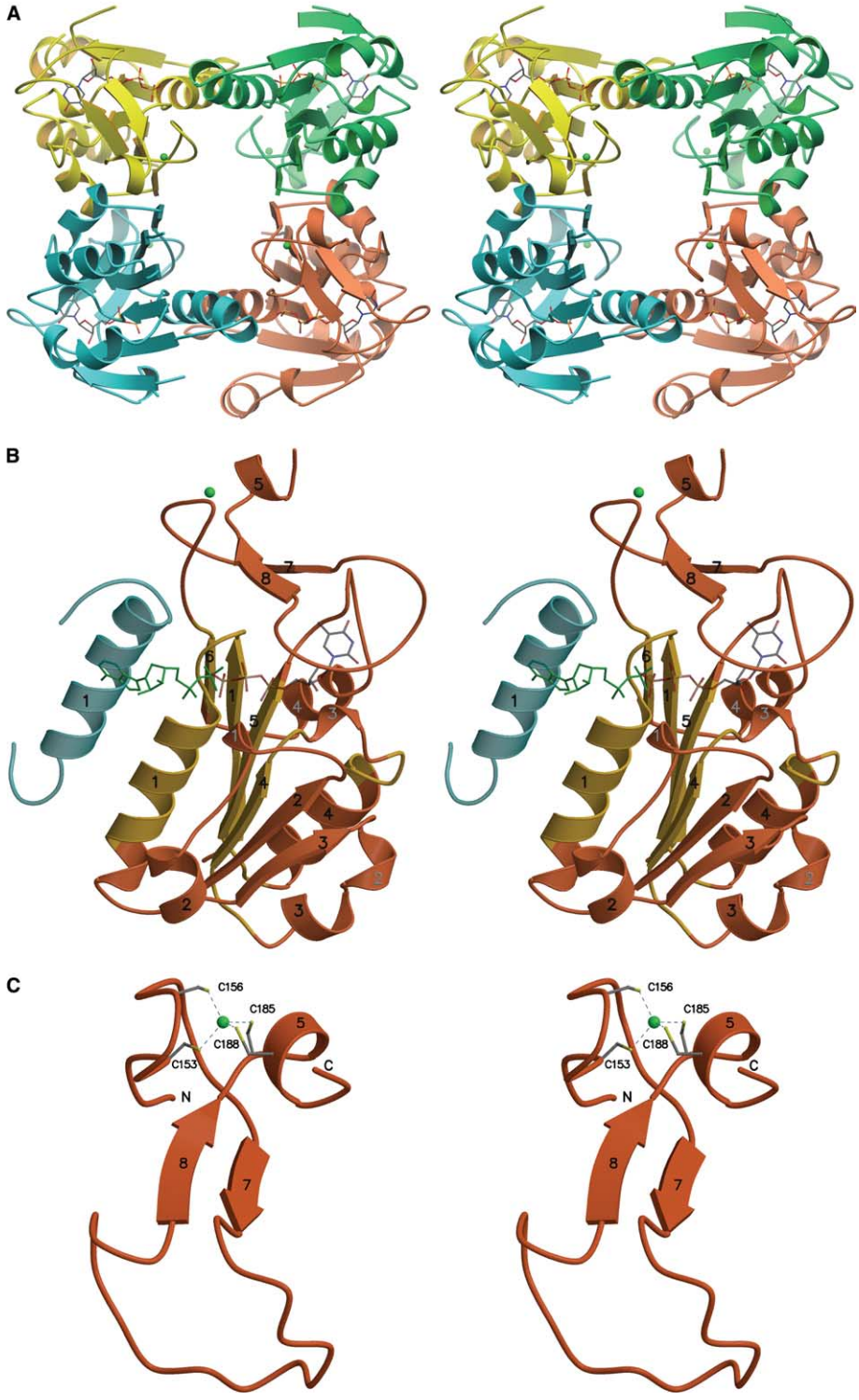

Fig. 2. Stereoview of hTK1 in complex with the feedback inhibitor dTTP. (A) Subunits A–D of the D_2-symmetric tetramer are shown in orange, cyan, yellow and green. The inhibitor dTTP is shown as ball and stick model (main conformation only). (B) Subunits A with modeled substrate ADP as taken from a superimposition with other nucleoside/nucleotide kinases [28]. This superposition is based on the yellow parts of the polypeptide consisting of four central β-strands with P-loop and one helix. The real position of the adenine of the ADP/ATP differs slightly avoiding the clash with the blue α-helix 1 from the neighbouring subunit. Secondary structure elements have been assigned by the program DSSP [20], α-helices and β-strands are numbered in black, 3_{10} helices are depicted with grey numbers. (C) The zinc-binding domain consists of the residues 150 (N) to 191 (C). The zinc ion is complexed by four cysteine side chains namely Cys 153, 156, 185 and 188.

The subunit arrangement in the tetramer is depicted in Fig. 2. Subunits A and B (as well as C–D, E–F, and G–H) form a dimer at the long helix α1 (Fig. 2).

The Zinc binding domain spans from residues 150 to 191. The metal binding motif formed by cysteines 153, 156, 185 and 188 accommodates a zinc ion (Fig. 2C), which was first

Table 1
Data collection and refinement statistics

Data set	dTTP:hTK1
Diffraction data[a]	
X-ray source	X06SA (SLS Villigen/CH)
Unit cell dimensions (Å)	a = 157.5; b = 122.9; c = 115.3; $\alpha = \gamma = 90°$; $\beta = 130.0°$
Resolution range (Å)	20.0–1.83 (1.95–1.83)
Completeness (%)	99.5 (99.8)
Multiplicity	7.1 (7.1)
Unique reflections	147503 (25536)
$R_{sym\text{-}I}$ (%)	8.4 (39.4)
I/σ	17.1 (7.9)
Space group	C2
Protomers per ASU	8
Wavelength (Å)	0.97934
Refinement and final model	
R_{cryst}/R_{free} (%)	15.9 /18.9
Number of reflections in working set	140080 (10345)
Number of reflections in test set	7423 (542)
Number of non-H-atoms	
Polypeptide	10106
dTTP atoms	232
Water molecules	774
Dithiothreitol atoms	8
Average B-factors (Å^2)	
All atoms	29.0
Polypeptide atoms	27.9
Main chain	26.0
Side chain	29.9
dTTP molecules	43.5
Water molecules	39.5
Dithiothreitol molecule	53.1
Rmsd from ideal geometry	
Bond lengths (Å)	0.016
Angles (°)	1.7
Ramachandran angles:	
Favored regions (%)	93.8
Allowed regions (%)	6.2

[a]The data were collected at 100 K. Values in parentheses are for the outermost shell.

detected by a fluorescence scan at the synchrotron (data not shown). Anomalous diffraction at the K-zinc edge was used for phase determination. Two cysteines are positioned before β-strand 7 and the other two after β-strand 8. Together with the antiparallel β-sheet formed by β-strand 7 and β-strand 8, the zinc bound to the cysteines seems to be crucial for the formation of the nucleoside binding site by stabilizing the conformation of the rather flexible loop (Leu166-Lys180) (Fig. 4), which is involved in nucleoside binding (Figs. 2c, 3). This cysteine motif –Cys–X–X–Cys–Z–Cys–X–X–Cys– is conserved for all enzymes of the type II subfamily as shown in the alignment (Fig. 1). In *M. pneumoniae* and *S. aureus*, however, the last cysteine is replaced by a histidine. The number of residues between the second and third cysteine is generally Z = 28 besides *L. major* and *M. pneumoniae* with Z = 29 and *S. aureus* and *B. anthracis* with Z = 34. The metal binding motif resembles the zinc binding motif of adenylate kinases of gram-positive bacteria [27].

The active center of the enzyme is defined by the bound feedback inhibitor dTTP observed in each of the subunits (Fig. 2A). Two slightly different binding conformations were found with an occupancy of 40% and 60%, respectively (Fig. 3A). Apart from the β-phosphate, that assumes two opposite positions in space, the two conformations are almost superimposed as shown in Fig. 3A. Presumably, the β-phosphate is at the place where the catalytic phosphoryl group transfer occurs as observed with adenylate kinase. Therefore a major mobility may expected explaining the observed two different position of the β-phosphate. Thymine is tied by a hydrogen bond network to the polypeptide backbone namely O4 with amide N of Phe128, O2 with amide N of Val174 and N3 with carbonyl oxygen of Val172. Moreover, it stacks between Phe101, Phe133 and Tyr181 (Fig. 3B). The C5 of thymine contacts Thr163. The ribose moiety of dTTP is depicted in its South (3′-*exo*/2′-*endo*) conformation and held in a hydrophobic environment formed by Met28, Phe101 and Leu124 and stabilized by hydrogen bonds. The γ-phosphoryl group of dTTP binds the P-loop with its sequence fingerprint –G–P–M–F–S–G–K–S– which is highly conserved for the type II subfamily. Its sequence differs slightly from the P-loop of the type I enzymes [24] while maintaining the same function. The P-loop (Gly26 to Ser33) forms a giant anion hole that binds the β-phosphate of ATP tightly in order to transfer the γ-phosphoryl group onto dT in the catalyzed reaction [28]. The catalytic residues Lys32 of the P-loop, that is assumed to be responsible for the transfer of the γ-phosphate from ATP to 5′-OH-group of dT, and Glu98, that acts as a base accepting the proton of the 5′-OH-group of dT in the ester forming reaction, are structurally conserved and present in all nucleoside/nucleotide kinases [25].

In the active center of hTK1 a hydrogen bonding network binds thymine to the backbone of the protein. This binding mode of thymine is in contrast to the one observed within the type I enzymes [29] and most other nucleoside/nucleotide kinases [30–32] which bind it via side chains. In the Herpes type I thymidine kinase Gln125 forms two hydrogen bonds to thymine. This glutamine is able to adapt to the different substrates like ganciclovir and 2′-deoxycytidine and their specific hydrogen-bond donor acceptor pattern by flipping its amide [33]. Such an adaptation is clearly not possible if the backbone of the protein is involved as in hTK1. In the case of 2′-deoxycytidine that has a comparable size to dT, the presence of the amino group with hydrogen-bond donor character at the place of the O4 (hydrogen-bond acceptor) of dT causes repulsion with the amide N of Phe128. The aromatic residues Phe101, Phe133 and Tyr181 are squeezing the base from opposite directions. This arrangement is similar to Phe96 and Phe137 of human deoxycytidine kinase but differs from the stacking of Met128 and Tyr172 in the Herpes enzyme [25]. These findings explain the difference in substrate acceptance observed between the nucleoside/nucleotide kinases. Substrate acceptance decreases from the Herpes TK having the broadest one, over human deoxycytidine kinase, human uridine cytidine kinase [32] to hTK1 with the narrowest one [25].

This major difference in binding mode among type I and II subfamilies accounts for the narrow substrate acceptance and higher specificity of hTK1 exploited for selective antiviral therapy. Furthermore, Thr163 points directly towards the C5 of the base restricting additionally the space availability and leaving no space for modifications at this position compared to the Herpes enzyme. This explains the rejection of 5-bromovinylde-

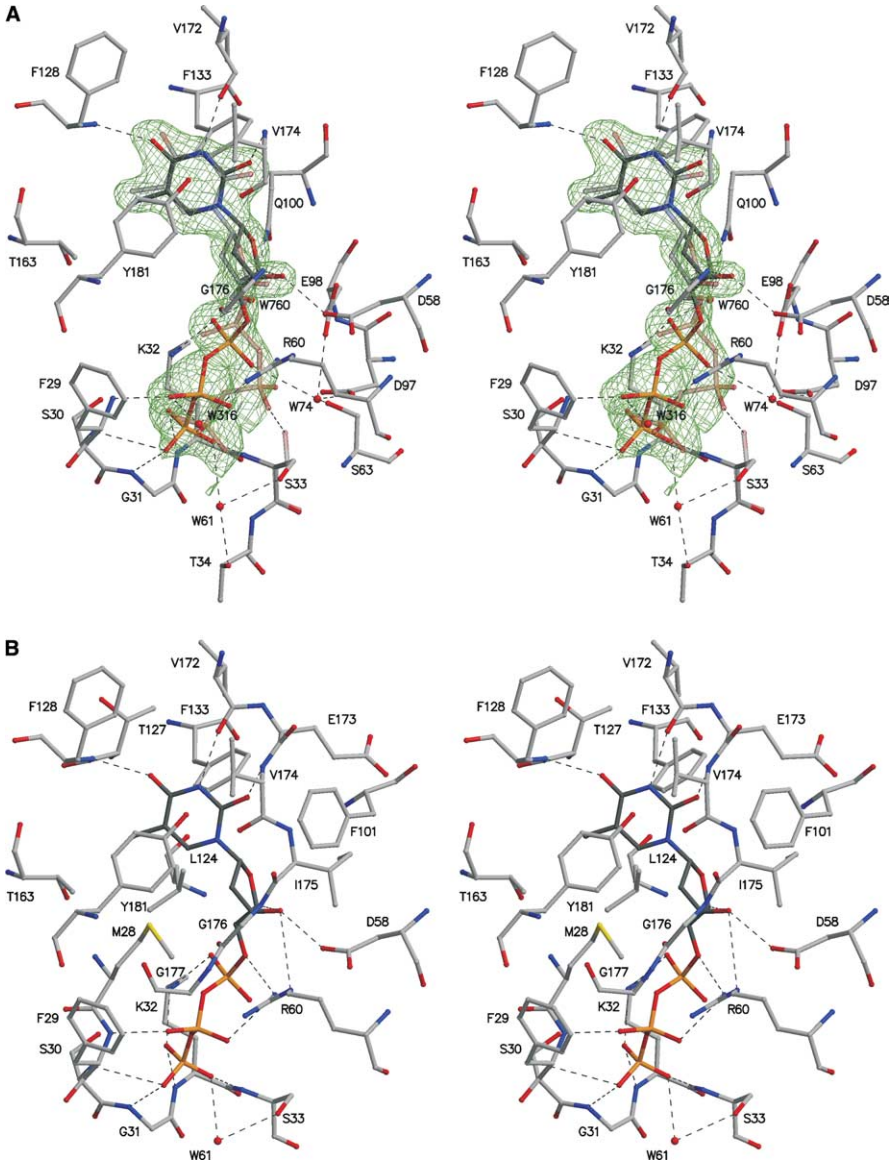

Fig. 3. Stereoview of the active center of hTK1. Water molecules are red balls, hydrogen bonds are dashed lines. (A) Bound feedback inhibitor dTTP with hydrogen bonding network. The conformation of dTTP in its two binding modes was derived from the F_o–F_c omit electron density map here contoured at 3σ (green). The 40% binding mode is shown in a semi transparent mode. (B) The nucleotide is bound by the tight interactions with protein residues. Hydrogen bonds to main chain atoms and stacking of the pyrimidine ring between Phe101, Phe133 and Tyr181 are responsible for the high substrate specificity.

oxyuridine [34]. The surrounding amino acids of the 3′-position of the ribose form a cleft between Asp58 and Ile175. This allows the accommodation of bulkier groups replacing the 3′-hydroxyl as for example the azido moiety of the prodrug AZT that is accepted as a substrate.

The observed structure suggests that Glu98 acts as a base accepting the proton of the 5′-OH-group of dT in the ester forming reaction corresponding to Glu83 of the Herpes enzyme [29]. Arg60 fixes the phosphate of the product dTMP which is at the position of the α-phosphate of dTTP in the reported structure. The position of the β-phosphate of dTTP corresponds to the γ-phosphate position of ATP which is transferred to dT. In the Herpes thymidine kinase like in numerous other nucleoside/nucleotide kinases the adenine of ATP is hydrogen bonded to the backbone oxygen of Gln331 situated at the N-terminus of an α-helix and interacts with Arg216 in a common stacking mode from one side while the other side is exposed to solvent. In hTK1 the helix binding the adenine moiety of ATP is missing in the monomer of hTK1. However a corresponding helix is found at the dimer interface between subunits A and B as well as C and D shown in Fig. 2B. This helix contains Arg41 in a suitable position to interact with the adenine. This indicates further that subunits A and B together are constituting a canonical active site, whereas subunits B and C do not complement each other. Thus, the dimer A–B is most likely the physiologically relevant one. This is in agreement with the fact that the truncated form of hTK1 is a dimer in solution and is catalytically fully active (Supplementary material Fig. S6 and Fig. S7). Catalytic activity cannot be expected from the alternative dimer B–C although it harbors a slightly larger interface.

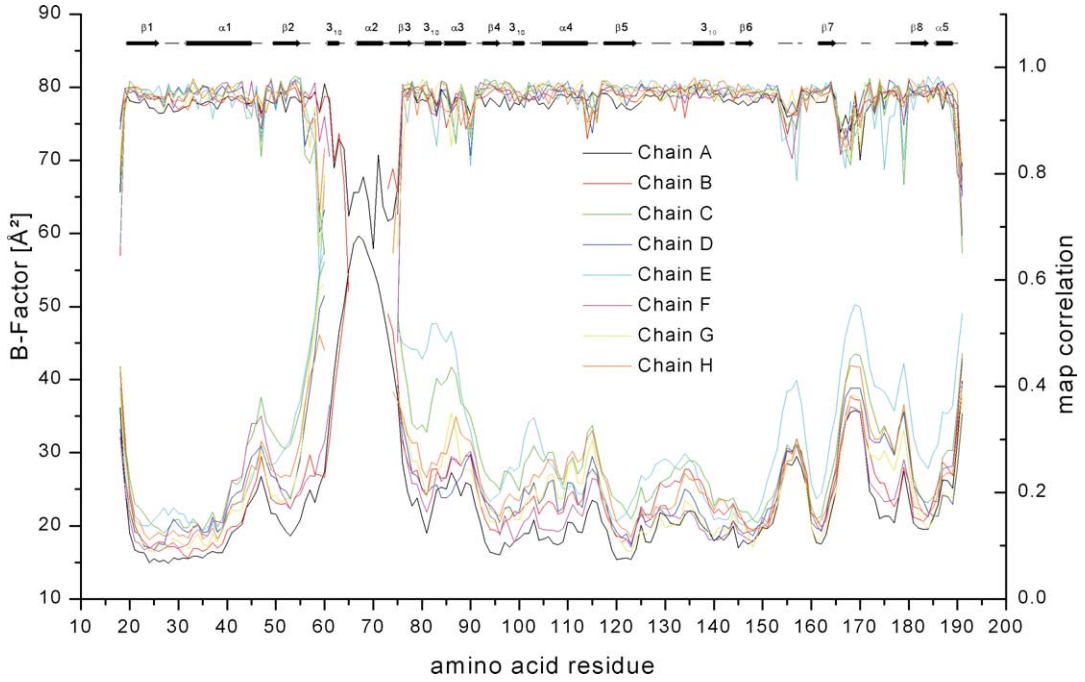

Fig. 4. B-factor plot of the eight subunits of the reported hTK1 structure. The map correlation is depicted on the right side of the diagram. High mobility of some residues leads to lacking parts in the structure. The line on top shows the secondary structure assignment as given by the program DSSP [20]. The β-sheets and helices are displayed as arrows and tubes, respectively and labeled.

The alignment of hTK1 with the orthologs from several pathogens indicates that rather accurate models can be produced because of a high homology. Nevertheless, the binding site may slightly differ because some of the residues involved in van der Waals contacts to thymidine are only partially conserved (Fig. 1). The structural knowledge on these differences can be exploited to generate new ideas for the synthesis of modified nucleosides towards the development of pathogen-specific prodrugs. The structure of hTK1 indicates that it is possible to add bulkier groups at the 3′-position of the sugar and/or at the C5-position of the base and that blocking the sugars in the North (2′-*exo*/3′-*endo*) or South (3′-*exo*/2′-*endo*) conformation is suitable for achieving selectivity towards the TK of the pathogens [35]. The substrate specificity of hTK1 may be broadened by mutating residues surrounding the ribose so that prodrugs with increased modifications at the sugar mimicking moiety may be processed [35] and in general by increasing space availability within the binding site. A first example of mutation is represented by Vaccinia Virus TK (VVTK). In VVTK, Thr163 of hTK1 is replaced by Ser (Ser148) while all other amino acids involved in dT binding are conserved (Fig. 1). In contrast to hTK1 [35], VVTK is able to phosphorylate (south)-methanocarbathymidine (Supplementary material Fig. S8). For the design of hTK1 inhibitors, the structural knowledge around the 5′ position of dT and around the phosphate of dTMP can be exploited to confer favorable pharmacodynamic and pharmacokinetic characteristics. The cleft near the 3′-position of the ribose is the most favorable region for inserting bulkier groups in novel PET tracers complementing ^{18}F-labeled dT. Unambiguously, different pharmaceutical fields of application will profit from the structural insights revealed by the presented structure of hTK1.

Acknowledgements: We thank T. Tomizaki from Swiss Light Source (Villigen, Switzerland) for his technical support and A. Limacher for help in collecting data sets at the beamline. We are grateful to R. Perozzo for helpful comments on the laboratory work. This work was supported by the Deutsche Forschungsgemeinschaft under SFB-388 and by the European Community (QLK3-CT-2001-01265). This work was performed at the Swiss Light Source, Paul Scherrer Institut, Villigen, Switzerland.

Appendix A. Supplementary data

Supplementary data associated with this article can be found, in the online version at doi:10.1016/j.febslet.2005.01.034.

References

[1] Arner, E.S. and Eriksson, S. (1995) Mammalian deoxyribonucleoside kinases. Pharmacol. Ther. 67, 155–186.
[2] Vogt, J., Perozzo, R., Pautsch, A., Prota, A., Schelling, P., Pilger, B., Folkers, G., Scapozza, L. and Schulz, G.E. (2000) Nucleoside binding site of herpes simplex type 1 thymidine kinase analyzed by X-ray crystallography. Proteins 41, 545–553.
[3] Elion, G.B., Furman, P.A., Fyfe, J.A., de Miranda, P., Beauchamp, L. and Schaeffer, H.J. (1977) Selectivity of action of an antiherpetic agent, 9-(2-hydroxyethoxymethyl) guanine. Proc. Natl. Acad. Sci. USA 74, 5716–5720.
[4] Oliver, F.J., Collins, M.K. and Lopez-Rivas, A. (1997) Overexpression of a heterologous thymidine kinase delays apoptosis induced by factor deprivation and inhibitors of deoxynucleotide metabolism. J. Biol. Chem. 272, 10624–10630.
[5] Hallek, M., Wanders, L., Strohmeyer, S. and Emmerich, B. (1992) Thymidine kinase: a tumor marker with prognostic value for non-

Hodgkin's lymphoma and a broad range of potential clinical applications. Ann. Hematol. 65, 1–5.
[6] Shields, A.F., Grierson, J.R., Dohmen, B.M., Machulla, H.J., Stayanoff, J.C., Lawhorn-Crews, J.M., Obradovich, J.E., Muzik, O. and Mangner, T.J. (1998) Imaging proliferation in vivo with [F-18]FLT and positron emission tomography. Nat. Med. 4, 1334–1336.
[7] Cobben, D.C., Jager, P.L., Elsinga, P.H., Maas, B., Suurmeijer, A.J. and Hoekstra, H.J. (2003) 3′-18F-fluoro-3′-deoxy-L-thymidine: a new tracer for staging metastatic melanoma?. J. Nucl. Med. 44, 1927–1932.
[8] Kohn, D.B., Sadelain, M., Dunbar, C., Bodine, D., Kiem, H.P., Candotti, F., Tisdale, J., Riviere, I., Blau, C.A., Richard, R.E., Sorrentino, B., Nolta, J., Malech, H., Brenner, M., Cornetta, K., Cavagnaro, J., High, K. and Glorioso, J. (2003) American Society of Gene Therapy (ASGT) ad hoc subcommittee on retroviral-mediated gene transfer to hematopoietic stem cells. Mol. Ther. 8, 180–187.
[9] Bonini, C., Ferrari, G., Verzeletti, S., Servida, P., Zappone, E., Ruggieri, L., Ponzoni, M., Rossini, S., Mavilio, F., Traversari, C. and Bordignon, C. (1997) HSV-TK gene transfer into donor lymphocytes for control of allogeneic graft-versus-leukemia. Science 276, 1719–1724.
[10] Verzeletti, S., Bonini, C., Marktel, S., Nobili, N., Ciceri, F., Traversari, C. and Bordignon, C. (1998) Herpes simplex virus thymidine kinase gene transfer for controlled graft-versus-host disease and graft-versus-leukemia: clinical follow-up and improved new vectors. Hum. Gene Ther. 9, 2243–2251.
[11] Kabsch, W. (1993) Automatic processing of rotation diffraction data from crystals of initially unknown symmetry and cell constants. J. Appl. Crystallogr. 26, 795–800.
[12] Brunger, A.T., Adams, P.D., Clore, G.M., DeLano, W.L., Gros, P., Grosse-Kunstleve, R.W., Jiang, J.S., Kuszewski, J., Nilges, M., Pannu, N.S., Read, R.J., Rice, L.M., Simonson, T. and Warren, G.L. (1998) Crystallography & NMR system: a new software suite for macromolecular structure determination. Acta Crystallogr. D 54, 905–921.
[13] de la Fortelle, E. and Bricogne, G. (1997) Maximum-likelihood heavy-atom parameter refinement for multiple isomorphous replacement and multiwavelength anomalous diffraction methods. Meth. Enzymol. 276, 472.
[14] Terwilliger, T.C. (2003) Automated main-chain model building by template matching and iterative fragment extension. Acta Crystallogr. D 59, 38.
[15] McRee, D.E. (1999) XtalView/Xfit-A versatile program for manipulating atomic coordinates and electron density. J. Struct. Biol. 125, 156–165.
[16] Collaborative Computational Project (1994) The CCP4 suite: Programs for protein crystallography. Acta Crystallogr. D 50, 760–763.
[17] Laskowski, R.A., MacArthur, M.W., Moss, D.S. and Thornton, J.M. (1993) PROCHECK: a program to check the stereochemical quality of protein structures. J. Appl. Crystallogr. 26, 283–291.
[18] Hooft, R.W., Vriend, G., Sander, C. and Abola, E.E. (1996) Errors in protein structures. Nature 381, 272.
[19] Fenn, T.D., Ringe, D. and Petsko, G.A. (2003) POVScript+: a program for model and data visualization using persistence of vision ray-tracing. J Appl. Crystallogr. 36, 944–947.
[20] Kabsch, W. and Sander, C. (1983) Dictionary of protein secondary structure: pattern recognition of hydrogen-bonded and geometrical features. Biopolymers 22, 2577–2637.
[21] Jones, Y. and Stuart, D. (1991) Proceedings of CCP4 Study Weekend on Isomorphous Replacement and Anomalous Scattering. Proceedings of CCP4 Study Weekend, 39–48.
[22] Munch-Petersen, B., Cloos, L., Jensen, H.K. and Tyrsted, G. (1995) Human thymidine kinase 1. Regulation in normal and malignant cells. Adv. Enzyme Regul. 35, 69–89.
[23] Lee, L.S. and Cheng, Y. (1976) Human deoxythymidine kinase II: substrate specificity and kinetic behavior of the cytoplasmic and mitochondrial isozymes derived from blast cells of acute myelocytic leukemia. Biochemistry 15, 3686–3690.
[24] Wild, K., Bohner, T., Aubry, A., Folkers, G. and Schulz, G.E. (1995) The three-dimensional structure of thymidine kinase from herpes simplex virus type 1. FEBS Lett. 368, 289.
[25] Eriksson, S., Munch-Petersen, B., Johansson, K. and Eklund, H. (2002) Structure and function of cellular deoxyribonucleoside kinases. Cell Mol. Life Sci. 59, 1327–1346.
[26] Schulz, G.E., Müller, C.W. and Diederichs, K. (1990) Induced-fit movements in adenylate kinases. J. Mol. Biol. 213, 627–630.
[27] Gilles, A.M., Glaser, P., Perrier, V., Meier, A., Longin, R., Sebald, M., Maignan, L., Pistotnik, E. and Barzu, O. (1994) Zinc, a structural component of adenylate kinases from gram-positive bacteria. J. Bacteriol. 176, 520–523.
[28] Abele, U. and Schulz, G.E. (1995) High-resolution structures of adenylate kinase from yeast ligated with inhibitor Ap5A, showing the pathway of phosphoryl transfer. Protein Sci. 4, 1262–1271.
[29] Wild, K., Bohner, T., Folkers, G. and Schulz, G.E. (1997) The structures of thymidine kinase from herpes simplex virus type 1 in complex with substrates and a substrate analogue. PG - 2097-106. Protein Sci. 6, 2097–2106.
[30] Johansson, K., Ramaswamy, S., Ljungcrantz, C., Knecht, W., Piskur, J., Munch-Petersen, B., Eriksson, S. and Eklund, H. (2001) Structural basis for substrate specificities of cellular deoxyribonucleoside kinases. Nat. Struct. Biol. 8, 616–620.
[31] Sabini, E., Ort, S., Monnerjahn, C., Konrad, M. and Lavie, A. (2003) Structure of human dCK suggests strategies to improve anticancer and antiviral therapy. Nat. Struct. Biol. 10, 513–519.
[32] Suzuki, N.N., Koizumi, K., Fukushima, M., Matsuda, A. and Inagaki, F. (2004) Structural basis for the specificity, catalysis, and regulation of human uridine-cytidine kinase. Structure 12, 751–764.
[33] Bennett, M.S., Wien, F., Champness, J.N., Batuwangala, T., Rutherford, T., Summers, W.C., Sun, H., Wright, G. and Sanderson, M.R. (1999) Structure to 1.9 A resolution of a complex with herpes simplex virus type-1 thymidine kinase of a novel, non-substrate inhibitor: X-ray crystallographic comparison with binding of aciclovir.PG - 121-5. FEBS Lett. 443, 121.
[34] Eriksson, S., Kierdaszuk, B., Munch-Petersen, B., Oberg, B. and Johansson, N.G. (1991) Comparison of the substrate specificities of human thymidine kinase 1 and 2 and deoxycytidine kinase toward antiviral and cytostatic nucleoside analogs. Biochem. Biophys. Res. Commun. 176, 586–592.
[35] Schelling, P., Claus, M.T., Johner, R., Marquez, V.E., Schulz, G.E. and Scapozza, L. (2004) Biochemical and structural characterization of (South)-methanocarbathymidine that specifically inhibits growth of herpes simplex virus type 1 thymidine kinase-transduced osteosarcoma cells. J. Biol. Chem. 279, 32832–32838.